1.14Tb/s DP-QPSK WDM polarization-diverse optical phase conjugation

M. F. C. Stephens,[*] **M. Tan, I. D. Phillips, S. Sygletos, P. Harper and N. J. Doran**

Aston Institute of Photonic Technologies, Aston University, Aston Triangle, Birmingham B4 7ET, UK
[*]*m.stephens@aston.ac.uk*

Abstract: Optical phase conjugation (OPC) of a polarization-multiplexed comb of 10x114Gb/s DP-QPSK signals has been demonstrated for the first time, occupying a spectral bandwidth of >1THz (~9nm). The nonlinear element employed for the OPC was highly nonlinear fiber (HNLF) optimized for the suppression of stimulated Brillouin scattering (SBS) and configured in a bi-directional loop offering polarization diversity. Pump power (each way about the loop) and input signal power to the OPC subsystem were optimized at 29.7dBm and + 3dBm respectively producing a Q^2 penalty of ≤0.9dB over all conjugate wavelengths, polarizations and output OSNR (up to 20dB).

©2014 Optical Society of America

References and links

1. A. Yariv, D. Fekete, and D. M. Pepper, "Compensation for channel dispersion by nonlinear optical phase conjugation," Opt. Lett. **4**(2), 52–54 (1979).
2. M. H. Chou, J. Hauden, M. A. Arbore, and M. M. Fejer, "1.5- μm -band wavelength conversion based on difference-frequency generation in LiNbO₃ waveguides with integrated coupling structures," Opt. Lett. **23**(13), 1004–1006 (1998).
3. R. Stolen, "Phase-matched-stimulated four-photo mixing in silica-fiber waveguides," IEEE J. Quantum Electron. **11**(3), 100–103 (1975).
4. G. P. Agrawal, "Four-wave mixing and phase conjugation in semiconductor laser media," Opt. Lett. **12**(4), 260–262 (1987).
5. F. Favre and D. Le Guen, "Four-wave mixing in traveling-wave semiconductor laser amplifiers," IEEE J. Quantum Electron. **26**(5), 858–864 (1990).
6. S. L. Jansen, D. van den Borne, P. M. Krummrich, S. Spalter, G. D. Khoe, and H. de Waardt, "Long-Haul DWDM transmission systems employing optical phase conjugation," IEEE J. Sel. Top. Quantum Electron. **12**(4), 505–520 (2006).
7. S. Watanabe, S. Takeda, and T. Chikama, "Interband wavelength conversion of 320 Gb/s (32×10 Gb/s) WDM signal using a polarization insensitive fiber four-wave mixer," Proceedings of ECOC **3**, 85–87 (1998).
8. D. Nesset, M. F. C. Stephens, A. E. Kelly, C. Gilbertas, J. Reed, K. A. Williams, S. Bouchoule, R. Kashyap, A. D. Ellis, and D. G. Moodie, "40 Gbit/s transmission over 186.6 km of installed fiber using mid-span spectral inversion for dispersion compensation," in *Proceedings of OFC* (1999), **3**, 118–120.
9. S. Takasaka, M. Takahashi, Y. Mimura, M. Tadakuma, R. Sugizaki, and T. Yagi, "Polarization insensitive arbitrary wavelength conversion in entire C-band using a PM-HNLF," in *Proceedings of ECOC* (2010), Th.9.C.2.
10. W. Forysiak and N. J. Doran, "Reduction of Gordon-Haus jitter in soliton transmission systems by optical phase conjugation," J. Lightwave Technol. **13**(5), 850–855 (1995).
11. M. Morshed, L. B. Du, B. Foo, M. D. Pelusi, and A. J. Lowery, "Optical Phase Conjugation for Nonlinearity Compensation of 1.21-Tb/s Pol-Mux Coherent Optical OFDM," in *Proceedings of OECC* (2013), PD3–4.
12. J. B. Coles, B. P.-P. Kuo, N. Alic, S. Moro, C.-S. Bres, J. M. Chavez Boggio, P. A. Andrekson, M. Karlsson, and S. Radic, "Bandwidth-efficient phase modulation techniques for Stimulated Brillouin Scattering suppression in fiber optic parametric amplifiers," Opt. Express **18**(17), 18138–18150 (2010).
13. K. Shiraki, M. Ohashi, and M. Tateda, "SBS Threshold of a Fiber with a Brillouin Frequency Shift Distribution," J. Lightwave Technol. **14**(1), 50–57 (1996).
14. J. M. C. Boggio, J. D. Marconi, and H. L. Fragnito, "Experimental and numerical investigation of the SBS threshold increase in an optical fiber by applying strain distributions," J. Lightwave Technol. **23**(11), 3808–3814 (2005).
15. K. K. Y. Wong, M. E. Marhic, K. Uesaka, and L. G. Kazovsky, "Polarization-Independent Two-Pump Fiber-Optical Parametric Amplifier," IEEE Photon. Technol. Lett. **14**(7), 911–913 (2002).

16. L. Grüner-Nielsen, *et al.*, "A silica based highly nonlinear fiber with improved threshold for stimulated Brillouin scattering," in *Proceedings of ECOC* (2010), Tu.4.D3.
17. L. Grüner-Nielsen, *et al.*, "Silica-Based Highly Nonlinear Fibers with a High SBS Threshold," in *Proceedings of IEEE Winter Topicals* (2011), MD3.2.
18. I. D. Phillips, *et al.*, "Exceeding the Nonlinear-Shannon Limit using Raman Laser Based Amplification and Optical Phase Conjugation" in Proceedings of OFC (2014), M3C.

1. Introduction

Optical phase conjugation (OPC) is a well-known process whereby an optical signal is propagated through a nonlinear medium in the presence of a pump beam to create a 'phase conjugate' signal, typically at a shifted frequency/energy. The conjugate possesses the unusual property of having a mirrored frequency spectrum compared to the initial signal whilst maintaining the same temporal structure [1]. Within telecoms applications, the conjugating element is typically a nonlinear optical waveguide which can support three-wave mixing via the χ^2 susceptibility [2] and/or four-wave mixing via the χ^3 susceptibility [3]. Specific examples of OPC elements range from discrete semiconductor optical amplifiers/lasers [4, 5] to periodically-poled lithium niobate crystals (PPLN) [6] and specialty optical fibers such as highly nonlinear fiber (HNLF) [7]. In particular, HNLF offers numerous advantages as a passive medium which is easily spliced to standard single mode transmission fiber with low loss.

The majority of telecoms research has historically focused on using OPC for chromatic dispersion (CD) compensation via mid-span spectral inversion (MSSI) [1, 8]. Potentially wide optical signal bandwidths can be conjugated with high efficiency as long as sufficient phase matching is maintained between the waves interacting in the process [9], and the ultrafast ~fs response-time of the nonlinearity additionally offers transparency to signal modulation format. Moreover, OPC via MSSI also offers the prospect of nonlinear compensation [10], and with coherent detection and DSP algorithms now commonly compensating for CD and other linear transmission impairments, OPC is being re-examined as a potentially efficient technique for parallel compensation of multichannel nonlinearities such as cross-phase modulation (XPM) [11].

Two major hurdles exist in implementing practical HNLF-based OPC: the first is the fundamental requirement for the pump wave and the signal wave to be co-polarized for maximal interaction and hence signal-to-conjugate efficiency; the second is the onset of stimulated Brillouin scattering (SBS) at the optical pump power levels required for efficient conjugation. The SBS acts so as to substantially reflect input power once a threshold is reached and can additionally increase conjugate phase and amplitude noise unless mitigating techniques are employed. Techniques reported for SBS-mitigation include phase or frequency dithering (modulation) of the pump to spectrally broaden it relative to the SBS bandwidth [12] or alteration of the physical properties of the fiber itself (e.g. via core doping [13] or imparting strain/thermal gradients [14]) to disrupt the SBS buildup.

Polarization diverse OPC has been demonstrated in numerous ways, but typically with the common factor of creating orthogonal pump components which subsequently interact with the relevant component of the signal having a parallel polarization at a particular moment in time. This can be achieved in various ways by e.g. using two discrete orthogonal pumps [15], placing the nonlinear element in a loop with counter-propagating orthogonal pump/signal polarizations [6, 7, 11] or by employing a reflective Faraday rotator [9]. However, to the best of our knowledge these schemes have not been shown to be compatible with the semi-standardized format of dual-polarization (DP)-QPSK modulation.

For OPC to emerge as a cost effective compensation scheme in DWDM systems, it is imperative that it can operate over as wide a spectral bandwidth as possible to minimize the number of pump wavelengths/OPC bands required to cover the full transmission band. Although impressive recent progress has been reported demonstrating conjugation of a single narrowband (~150GHz) PM-OFDM 'superchannel' [11], there has been no demonstration of a wide bandwidth, polarization-diverse OPC conjugating multiple WDM PM-signals with coherent detection. We report here an OPC capable of conjugating >1THz (~9nm) optical

bandwidth and for the first time demonstrate conjugation of a 1.14Tb/s (10x114Gb/s) multiplex of DP-QPSK signals.

2. Experimental set-up

The experimental set-up is shown in Fig. 1. A bank of ten DFB lasers (100GHz-spaced) were set contiguously from 193.1THz (1552.12nm) to 192.2THz (1559.79nm) and multiplexed together. The DFBs were combined with a tuneable 100kHz linewidth laser which acted as "signal under test" during the measurement process whereby the appropriate DFB was switched off and the 100kHz laser tuned into the vacated space. The WDM multiplex was QPSK-modulated using normal and inverted 28.5Gbaud/s, 2^{31}-1 patterns with an 18bit relative delay to drive an IQ modulator, followed by a polarization multiplexing emulator (Pol. Mux.) with ~2ns delay between polarization states. The signals were optically amplified to 20dBm via EDFA1, the mid-stage of which contained 6km of SSMF to give a further ~15 symbol decorrelation over the WDM band. A wavelength selective switch (~5dB insertion loss) was used to remove out-of-band ASE from EDFA1 at the expected conjugate wavelengths, and a polarization controller (PC3) fitted when appropriate to explore the OPC dependence on input signal polarization.
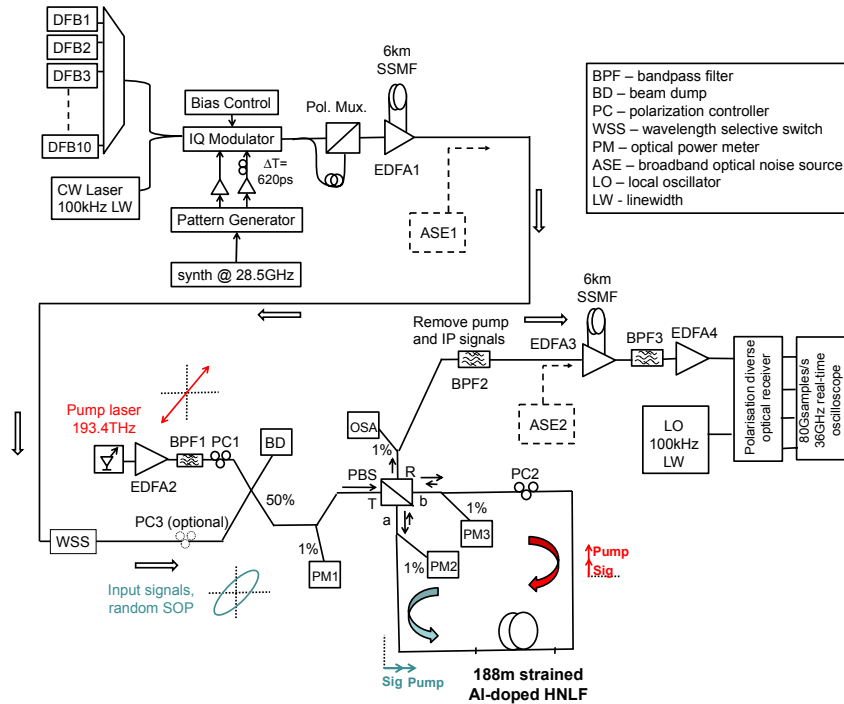

Fig. 1. Schematic of experimental set-up for polarization-diverse OPC.

The pump was obtained from a ~500kHz linewidth laser at 193.4THz (1550.1nm) and amplified via EDFA2 to ~40dBm (10W) before filtering by BPF1 (loss ~2dB, 3dB BW ~1nm) to remove ASE. The pump was combined with the signals via a 2x2 50% coupler (the unused arm of the coupler terminating at beam dump BD). Due to remnant ASE present close to the pump, the guard-band between pump and signals was set at a fairly conservative 300GHz (~2.4nm). It is anticipated that this spacing could be reduced with better filter design. The pump and randomly-polarized signals were routed to the transmissive port T of a 2x2 polarization beam splitter (PBS) which split both into two orthogonal "TE" and "TM" polarizations exiting ports a and b. These ports were respectively spliced to two ends of a

188m length of HNLF forming a bi-directional loop. A polarization controller PC2 was included to adjust the loop polarization.

The commercially-available HNLF had a loss of 2.6dB (including splices) and had been optimized to increase the stimulated Brillouin scattering (SBS) threshold, meaning that pump dithering could be avoided – a significant advantage of this approach in terms of experimental complexity and performance constraints. The HNLF [16] incorporated an aluminum-doped core and was linearly strained [17] from 100 to 1000g to produce an SBS threshold of ~1W. The nonlinear coefficient was 6.9 $(W.km)^{-1}$ and the zero dispersion wavelength (ZDW) λ_0 ranged from ~1552nm at 100g strain to ~1564nm at 1000g strain. The dispersion of the fiber was −0.19 ps/(nm.km) and the dispersion slope 0.024 ps/(nm^2.km) measured at 1550nm.

The pump polarization was controlled via PC1 to be as close to 45° linear as possible by both maximizing and equalizing the power measured on power meters PM2 and PM3. OPC occurred when a pump component mixed with a signal component sharing the same polarization and direction around the loop, producing two sets of orthogonal conjugates per wavelength which were subsequently re-combined at the PBS, exiting at the reflective port R. The power and overall shape of the conjugated spectrum at R could then be optimized using PC2. Ten 100GHz-spaced conjugates were generated between 193.7THz (1547.72nm) and 194.6THz (1540.56nm). The conjugates were isolated from the pump and original signals by a high-power tolerant wideband filter BPF2. It should be noted that PC1 and PC2 were 'set-and-forget' polarization controllers and the setup could be left stably for several hours after an initial adjustment period.

The receiver chain consisted of: amplifier EDFA3 containing 6km SSMF (to compensate for the SSMF used to de-correlate the data signals at the transmitter); a 100GHz filter BPF3 followed by EDFA4 to provide a constant + 4dBm conjugate power into a polarization diverse coherent receiver. The conjugate and a 100kHz linewidth local oscillator (+ 10dBm) were subsequently mixed together in a 90° optical hybrid before balanced detection which recovered the in-phase (I) and quadrature (Q) signals in the X- and Y- polarizations. The four signals were sampled and digitized using an 80Gs/s real-time oscilloscope with a 36 GHz analog bandwidth. The data was processed using off-line DSP which included signal normalization, low pass filtering, down-sampling, static dispersion compensation, local oscillator frequency offset compensation, clock recovery, polarization recovery (constant modulus algorithm) and phase recovery. Performance was characterized by measuring the Q-factor (Q^2) of the resulting constellation, and averaged over 570 kSymbols.

3. OPC optimization

Figures 2(a) and 2(b) show output spectra at port R for spectrally flat input signals and for two different settings of PC2. PC2 not only affected the transmitted power at R, but additionally introduced polarization-dependent spectral filtering of the output. This filtering was postulated to be due to the common-path interferometric arrangement of the HNLF loop.

In Fig. 2(a), PC2 was adjusted for overall spectral symmetry and maximum power for the conjugates closest to the pump. In Fig. 2(b), PC2 was adjusted for conjugate spectral-flatness which caused significantly reduced reflected pump power and flatness of the original signals due to the filtering effect described. Figure 2(b) additionally shows an increase in unwanted mixing products (visible between the conjugates and pump) which caused ~0.5dBQ performance degradation for all conjugates. The spectral shape was therefore set symmetrically in the Fig. 2(a) configuration for subsequent results.

Figure 2(c) illustrates the robustness of the conjugator to changes in input polarization via a systematic rotation of PC3. For each position/polarization, the Q^2 of the DP-QPSK conjugate at 193.7THz (1547.7nm) is plotted for an OSNR of 20dB. It should be noted that the Q^2 value is taken as the average of the estimated Q^2 for the two orthogonal components of the DP-QPSK signal. These are shown by way of example as X-pol and Y-pol in the inset constellation plots for two points. The variation in performance was small (std. dev. of

<0.1dB for this sample) and within natural fluctuation levels. No impact on Q^2 was observed due to strain-induced birefringence of the HNLF [17]. It is likely that any PMD produced via this mechanism was compensated for by the constant modulus algorithm of the DSP. The OPC can therefore be considered polarization diverse to polarization-multiplexed signals.
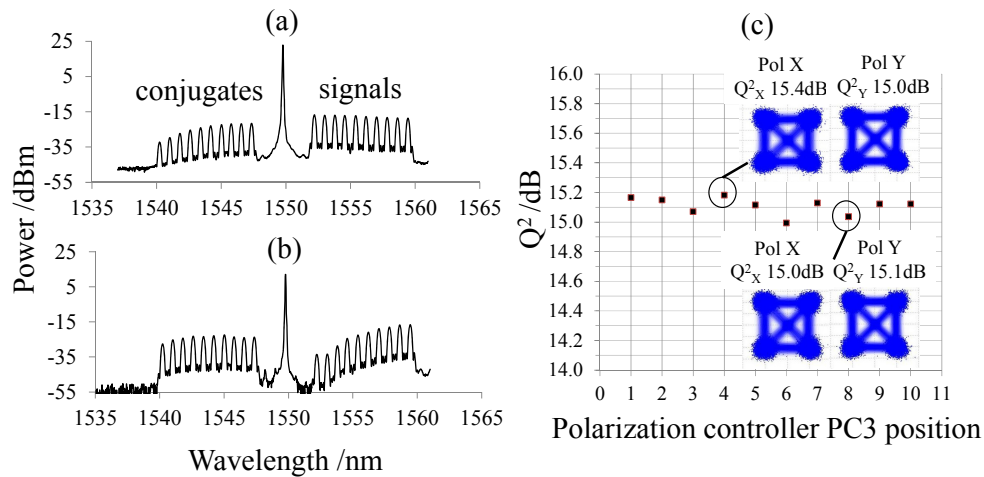

Fig. 2. (a) Spectrum at 'R' after PC2 adjusted for overall spectral symmetry (b) Spectrum at 'R' after PC2 adjusted for conjugate spectral flatness (c) Effect of input signal polarization on received Q^2 for ten different positions of PC3 for channel 193.7THz at 20dB OSNR.

An important consideration for optimizing the OPC was characterizing the pump power and input signal power per channel which offered the highest performance simultaneously over all 10 channels. Adjusting these powers influenced conjugate output power, spectral shape and importantly the level of crosstalk arising from 'unwanted' four-wave mixing products appearing at the conjugate wavelengths. The crosstalk level could only be measured by switching off an input signal (which in turn slightly changed the level of crosstalk that existed prior to the channel being removed).

Figures 3(a) and 3(b) display snapshots of the crosstalk at two different input signal launch powers of + 6dBm per channel and + 3dBm per channel respectively (measured after the WSS) as neighboring channels were sequentially removed. In both cases, the pump power was kept fixed at 29.7dBm into both ends of the HNLF loop, and the conjugate at 193.8THz (1546.9nm) also removed for viewing the crosstalk on both sides of conjugate 193.7THz (1547.7nm). It can be seen that the power of the mixing products was highly dependent on input signal power as expected, but also that the distribution of channels present greatly influenced the distribution of crosstalk power against wavelength. With so many mixing products existing, and dependent on multiple factors, it was outside the scope of this experiment to fully characterize the multi-dimensional parameter space, and it is suggested that this analysis is perhaps better suited to simulation. However, Fig. 3(c) shows the absolute power and power-delta of the crosstalk product at 193.8THz (1546.9nm) as sequential channels were removed. Please note that point for + 3dBm signal power with five channels removed is not plotted as it was within the system noise floor. The results show that a 3dB input power reduction from + 6dBm per channel to + 3dBm per channel with one channel removed lowered the power of the mixing product by 5.9dB due to the multiplicative nature of the crosstalk. Removing subsequent channels drops this difference to 4.1dB between the two powers which indicates a higher crosstalk contribution from directly neighboring channels at the higher + 6dBm input power. In the + 3dBm case, the crosstalk power remains approximately constant as the first three channels are removed, implying a greater relative contribution from the pump power under these conditions. It should be noted

that these trends would differ if presented for other crosstalk products (e.g. 193.6THz/1548.5nm).
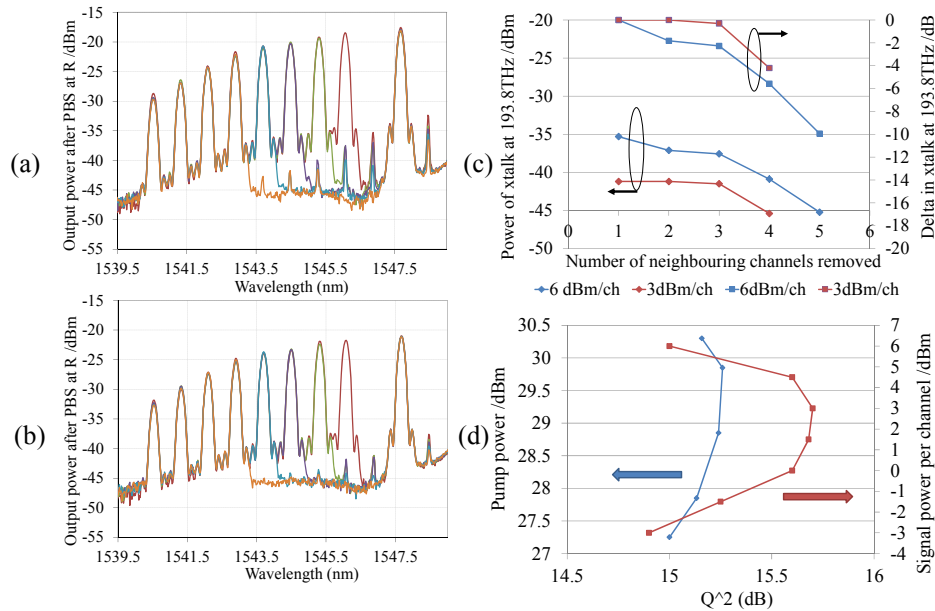

Fig. 3. (a) Snapshot conjugate spectra at 'R' for + 6dBm/ch input signal power, illustrating FWM crosstalk levels as neighboring channels removed (b) The same with + 3dBm/ch input signal power (c) Power and delta change of crosstalk product at 193.8THz (1546.9nm) as channels removed for + 6dBm/ch and + 3dBm/ch cases (d) Optimization of pump and input signal power per channel for the conjugate at 193.7THz (1547.7nm).

Because of the delay required for offline processing of Q^2, performance optimization over signal and pump power was performed for only one conjugate of the ten at 193.7THz (1547.7nm) and trends are displayed in Fig. 3(d). It can be seen that the OPC had a wide dynamic range of ~7.5dB with input signal power per channel (−2dBm/ch to + 5.5dBm/ch) for only 0.5dB Q^2 variation from peak performance. The optimum input signal power was found to be + 3dBm/ch (for a fixed pump power of 29.7dBm). Performance dropped off at high signal power due to enhanced inter-channel crosstalk from unwanted four wave mixing.

The performance trend with pump power was similar (with signal power kept fixed at + 3dBm/ch), showing optimum performance at a power of 29.7dBm in each direction around the HNLF loop. The drop with higher pump power is again attributed to increased four wave mixing, but also due to increased residual ASE from EDFA2 (pump power is raised by increasing the gain of EDFA2 which produced more ASE). The pump also began to exceed the SBS threshold of the HNLF at ~30dBm which may have limited performance at higher powers.

4. Q^2 vs OSNR performance

Figure 4 shows Q^2 against optical signal to noise ratio (OSNR) for all ten input signals and their corresponding conjugates as the OSNR was degraded after the OPC via broadband noise source ASE2 placed before the coherent receiver. The input signal power was set at + 3dBm per channel and the pump power was 29.7dBm in each direction about the HNLF loop. The inset to Fig. 4 shows the equivalent data expressed as a Q^2 penalty, with a linear trendline plotted. It can be seen that there was an OSNR-dependent Q^2-penalty for the conjugates with respect to the back-to-back performance. At low OSNR (12dB), the added ASE noise appeared to dominate performance, with the conjugates showing a negligible average penalty across all wavelengths of ~0.1dB. At higher OSNRs (20dB) the average

penalty increased to a mean of ~0.65dB, arising from both the unwanted four wave mixing products and residual/conjugated ASE. The reduced penalty observed at low OSNR allows the implementation of this OPC subsystem within a mid-span arrangement where the OSNR would be necessarily low. This is confirmed in a recent work using this arrangement which demonstrated a significant transmission distance improvement [18].
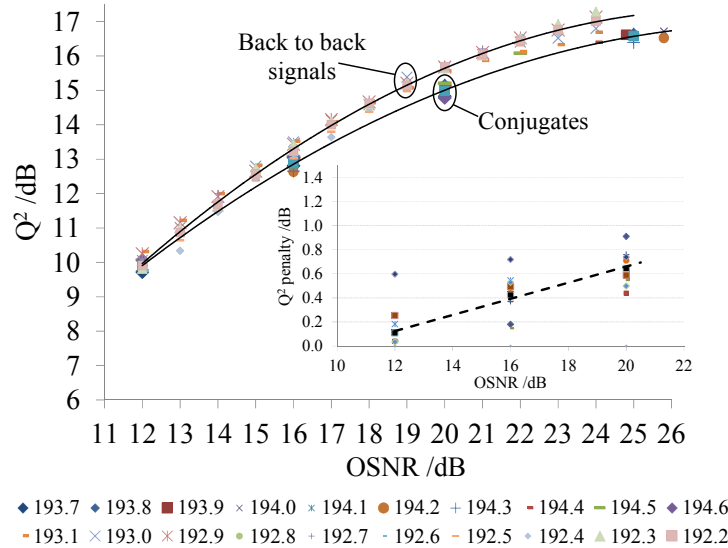

Fig. 4. Q^2 (dB) vs OSNR (dB) for 10x114Gb/s back-to-back signals and their respective conjugates. Inset shows the Q^2 penalty at three OSNR values from same data set.

It should be noted that Fig. 4 consistently shows the conjugate nearest the pump (193.7THz) suffering the largest penalty - rising from 0.6dB at 12dB OSNR to ~0.9dB at 20dB. It is believed that the main cause of this systematic result is residual ASE impacting the conjugate due to imperfect bandpass filtering after EDFA2. This penalty should be reduced towards the average by tighter filtering (e.g. using a fiber Bragg grating).

Figure 5 shows results with noise added <u>before</u> the OPC via noise source ASE1 to examine the OSNR degradation imparted by the conjugator – in this way, OPC conversion efficiency can be estimated for different input OSNR conditions (i.e. effectively an 'OPC noise figure'). The inset plot shows how the OSNR penalty varied with input OSNR for the key channels across the band. Conjugate OSNR was estimated using an optical spectrum analyzer to first measure the peak power of the conjugate under test and then by switching off the relevant signal/conjugate to measure the noise power at the conjugate wavelength in a resolution bandwidth of 0.1nm. The noise measurement therefore included the four-wave mixing products resulting from only the nine remaining signals, and produced a slightly different OSNR value from the actual ten-channel case. This was considered a reasonable approximation for examining the trends.

It can be seen from Fig. 5 that the outer conjugate 194.6THz (1540.6nm) consistently suffered the largest OSNR reduction at the relative large offset of 1.3THz from the pump. By shifting all the input signals up 100GHz (i.e. reducing the pump-signal guard-band by 100GHz) the peak power of the 'outer' conjugate would likely improve at the expense of increased ASE noise overlapping the nearest conjugate to the pump which would then be generated at 193.6THz (1548.5nm). Alternatively, the OPC bandwidth could be extended by employing a different HNLF with the average ZDW both more uniform (with fiber length), and closer to the pump wavelength. Additionally a lower dispersion and/or dispersion slope HNLF should also extend the OPC bandwidth.
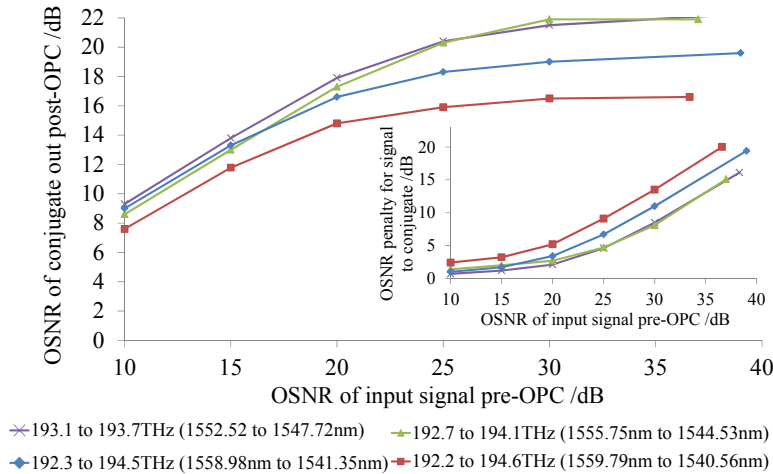
Fig. 5. Conjugate OSNR (dB) (measured post-OPC) vs input signal OSNR (dB) (measured pre-OPC) for four representative conjugates across the band. Inset shows OSNR penalty (dB) vs input signal OSNR (dB) for the same data set.

Figure 5 additionally shows the output OSNR of the OPC saturating as the input OSNR was increased, reaching a maximum output OSNR of ~22dB at 193.7THz (1547.7nm) for an input OSNR of 38dB. The saturation was due to a combination of factors including the fundamental signal-to-conjugate conversion efficiency of the HNLF and the noise floor of the system at the conjugate wavelengths which included not only direct remnant ASE noise from EDFA2 at the conjugate wavelengths, but also conjugated noise from all system EDFAs within the input signal band. The noise floor also included the crosstalk four-wave mixing terms, leading to a hard output OSNR limit. Figure 5 shows that as the input OSNR was lowered (e.g. to 10dB), the OSNR penalty was also significantly reduced to a minimum of 0.7dB for 193.7THz (conjugate nearest pump) and a maximum of 2.4dB for 194.6THz (conjugate furthest from pump).

4. Conclusions

Polarization-diverse optical phase conjugation of 10 x 114Gb/s 100GHz-spaced DP-QPSK signals with coherent detection was demonstrated and characterized for the first time using HNLF arranged in a bi-directional loop configuration. The variation of conjugate Q^2 with input signal polarization was shown to be very small (± 0.1dB), and provided robust operation over several hours without any form of external stabilization.

An OSNR dependent Q^2 penalty was observed rising from an average (across all conjugate wavelengths) of 0.1dB at 12dB OSNR to 0.65dB at 20dB OSNR. The maximum Q^2-penalty of 0.9dB was measured for the conjugate adjacent to the pump at an OSNR of 20dB, and it is believed that this degradation can be further reduced using tighter bandpass filtering after the high power EDFA used for pump amplification.

The OSNR degradation (effective noise figure) of the OPC was characterized for four conjugates across the band and was shown to be input-OSNR dependent (reduced input OSNR translating to reduced effective noise figure). For an input OSNR of 10dB, the worst-case OSNR degradation was found to be 2.4dB for the conjugate located furthest from the pump. This reduction in penalty for degraded input OSNR could aid mid-span spectral inversion applications, where OSNR is necessarily lower due to pre-transmission. It is anticipated that the OPC bandwidth can be extended using alternative HNLF with more suitable characteristics (ZDW uniformity, dispersion slope etc.) and also that conjugation of higher spectral efficiency modulation formats can be achieved.

Acknowledgments